

Seismic pulse propagation in 2-D and 3-D random media

Tobias M. Müller and Serge A. Shapiro¹

keywords: *Seismic waves, scattering, random media, generalized O'Doherty-Anstey formalism*

ABSTRACT

We consider the time evolution of seismic primary arrivals in single realizations of disordered structures. Using the Rytov approximation, we construct the Green's function of an initial plane wave propagating in 2-D and 3-D weakly heterogeneous fluids and solids. Our approach is a 2-D and 3-D extension of the dynamic-equivalent medium description of wave propagation in 1-D heterogeneous media, known also as generalized O'Doherty-Anstey formalism. The Green's function is constructed by using averaged logarithmic wavefield attributes and depends on the second order statistics of the medium heterogeneities. Green's functions constructed in this way, describe the primary arrivals in single typical realizations of seismograms. Similar to the attenuation coefficient and phase increment of transmissivities in 1-D, the logarithmic wavefield attributes in 2-D and 3-D also demonstrate the self-averaging, restricted however mainly to the weak fluctuation range. We show how to derive the statistical approximations and discuss their limitations. Further we compare the outcome of finite difference experiments with the theoretically predicted wavefield and find a good agreement: the presented statistical approximations give a smooth version of the primary arrivals. In addition, we formulate the travel-time corrected averaging from first principles. We discuss the relationship between our approach and approaches based on the travel-time corrected formalism. Strictly speaking, such approaches are not able to describe wavefields in typical realisations; the generalized O'Doherty-Anstey formalism however does it.

INTRODUCTION

In the recent years, the effect of multi-scale heterogeneities in earth-models has been recognized as a vital aspect of the overall behavior of seismic waves. Very much effort has been spent in the understanding of wave propagation in layered media.

¹**email:** tmueller@geophysik.fu-berlin.de

Especially seismic waves propagating in randomly multi-layered media are subjected to stratigraphic filtering. The physical reason is the multiple scattering by 1-D inhomogeneities. In random statistically homogeneous media, explicit approximations for the transmissivities of obliquely incident P- and SV-plane waves have been found by applying the second-order Rytov approximation to the 1-D multiple scattering problem in the frequency domain. This description is known as the generalized O'Doherty-Anstey formalism (Shapiro and Hubral, 1999).

However, the earth, the lithosphere and especially reservoirs may have a very complex geological structure including multi-scale 3-D heterogeneities. This becomes evident from geological surveys and horizontal well-log data. In such cases the concept of 2-D or 3-D random media is a more suitable and more general description. There are numerous studies that assume the earth as a realization of a random medium (see Sato and Fehler (1998) for an overview). The random medium consists of a constant background of a certain medium parameter – the reference medium – and its corresponding fluctuations, that is a realization of a statistically homogeneous random process in space. The latter is statistically characterized by a spatial correlation function. Crustal heterogeneities are best explained using an exponential (or more generally von Karman) correlation function which is rich in short-wavelength components.

Amplitudes and phases of wavefields fluctuate in random media. Typically, one can observe a spatial decay of propagating modes that depend on the ratio of wavelength to the characteristic size of heterogeneity. Furthermore, averaged wavefields are characterized by scattering attenuation and dispersion; both are important parameters for rock characterization. A suitable description of these wavefield characteristics enables the construction of Green's functions for heterogeneous media. The latter is extremely useful in order to apply – in combination with the usual macro-model – any kind of (true-amplitude) imaging or inversion technique, a fundamental problem in exploration seismics. For example, taking into account the small-scale heterogeneities of reflector overburdens improves AVO-analyses; this was clearly demonstrated for 1-D heterogeneities by Widmaier et al. (1996).

Common theories of wave propagation in random media predict average wavefield attributes for an ensemble of medium realizations. In geophysical practice, there is always one medium realization available. Therefore only a spatial averaging instead of ensemble-averaging can be performed. However, what should we do to describe non-averaged single seismograms? In order to use any averaged theoretical result for describing typical single seismograms we have to assume self-averaging of some wavefield attributes. This phenomenon is well studied in 1-D random media. Especially for transmission problems, logarithmic wavefield attributes turn out to be such self-averaged quantities (Lifshits et al., 1988, Shapiro and Hubral, 1999). We use this fact in the construction of the transmission response. We

will show later how the process of self-averaging works in 2-D and 3-D random media.

Due to scattering by the inhomogeneities the wavefield becomes distorted and can be described as a sum of coherent and incoherent wavefield (at least in the weak scattering range), where the coherent wavefield may be thought as a result of constructive interference of scattered waves (see Shapiro and Kneib, 1993). Which part of the wavefield is actually measured in experiments depends on the size of the receiver used. In geophysical applications the receivers are small compared with the wavelength and the size of inhomogeneities, so that the incoherent field will not be averaged out and the both parts of the wavefield participate in seismograms. That is for point-like receivers no aperture averaging, which reduces the fluctuations, take place. Therefore there may occur a discrepancy between the recorded wavefield and the coherent wavefield (or equivalently meanfield) (Wu, 1982). Formalisms that take into account these shortcomings and that try to improve the statistical averaging procedure to adopt it for seismology are based on heuristic assumptions like the travel-time corrected formalism (see for an overview Sato and Fehler, 1998).

There is, however, a lack of first principles, i.e., wave-equation-based descriptions of seismic pulse propagation which go beyond the meanfield theory and are valid for seismograms of single realizations of random media. This is exactly the motivation of this study. Our consideration is based on two theoretical studies of propagation of a pressure wavefield in 2-D and 3-D acoustic random media characterized by isotropic statistically homogeneous velocity fluctuations (see Shapiro and Kneib (1993) and Shapiro et al. (1996)). Here we present a description of the wavefield in a perturbation approximation, namely the Rytov approximation, which enables us to predict the transmitted wavefield around the primary arrivals in a typical single realization of a seismogram.

In analogy to the generalized O'Doherty-Anstey formalism for the 1-D case (Shapiro and Hubral, 1999), we call our description of the wavefield a dynamic-equivalent medium approach since it is applicable to a broad range of frequencies. Strictly speaking, our approach for 2-D and 3-D media is however not valid in the low frequency range, i.e. if the wavelength exceeds by far the characteristic size of heterogeneity. Thus, our approach is limited to the weak scattering range (the so-called unsaturated range), where multiple scattering with small scattering angles dominates. The Rytov approximation used in our approach is a powerful method in the weak fluctuation theory (Ishimaru, 1978).

The paper is organized as follows: First we give a short review of the results already obtained in the Rytov approximation, i.e., we consider a time-harmonic plane wave in an acoustic random media and derive the approximations for the wavefield attributes. It will be shown that logarithmic wavefield attributes related to the attenuation and the

phase velocity are self-averaged quantities. We numerically demonstrate the effect of self-averaging which enables us to compare our theoretical result with a typical single realization of a seismogram. Then we construct the Green's function based on these approximations for an acoustic random medium and discuss its validity range. After that we extend the approximations for the transmission response to the case of elastic random media; the construction of the Green's function is analogous. We confirm by finite difference modeling in 2-D elastic random media the obtained results.

THEORY

Time-harmonic plane waves in random media

It is known that the scattering of seismic waves in media with a large characteristic size of heterogeneity compared with the wavelength is confined within small angles around the forward direction. This means the conversion between P and S-waves in elastic media can be neglected. In other words, we can study scattering processes of P or S-waves in inhomogeneous media using the acoustic (scalar) wave equation. In the following, we look for a solution of the stochastic acoustic wave equation, which reads:

$$\Delta u(\mathbf{r}, t) - p^2(\mathbf{r}) \frac{\partial^2 u(\mathbf{r}, t)}{\partial t^2} = 0 \quad (1)$$

with $u(\mathbf{r}, t)$ as a scalar wave field (in the following simply denoted by u). Here we defined the squared slowness as

$$p^2(\mathbf{r}) = \frac{1}{c_0^2} (1 + 2n(\mathbf{r})) \quad , \quad (2)$$

where c_0 denotes the propagation velocity in a homogeneous reference medium. The function $n(\mathbf{r})$ is a realization of a stationary statistically isotropic random field with zero average ($\langle n(\mathbf{r}) \rangle = 0$); it describes approximately the velocity fluctuations since for $|n(\mathbf{r})| \ll 1$ we have

$$c(\mathbf{r}) \approx c_0(1 - n(\mathbf{r})) \quad . \quad (3)$$

Starting point for an analysis of acoustic scattering is the Lippmann-Schwinger equation, which is an integral solution to the scattering problem. Unfortunately, this is not an analytical closed representation and hence reduces its applications. One way to get around this problem is the linearization by a smooth perturbation approximation, often referred to as Rytov approximation (Ishimaru, 1978).

The Rytov method describes the wavefield fluctuations with help of the complex exponent

$$\Psi = \chi + i\phi \quad (4)$$

and develops a series solution of this quantity. The real part χ represents the fluctuations of the logarithm of the amplitude (log-amplitude fluctuations) and takes into account the scattering attenuation; the imaginary part ϕ represents phase fluctuations.

We consider a time-harmonic plane wave propagating in a 2-D and 3-D random medium. To be specific, we assume that the initially plane wave propagates vertically along the z-axis. We assume further that the wavefield inside the random medium can be described with help of the Rytov transformation (4) (the time dependence $\exp(-i\omega t)$ is omitted)

$$u(\mathbf{r}) = u_0(\mathbf{r}) \exp(\chi(\mathbf{r}) + i\phi(\mathbf{r})) \quad , \quad (5)$$

where $u_0 = A_0 \exp(i\phi_0)$ is the wavefield in the reference medium, A_0 is the amplitude and ϕ_0 its unwrapped phase. Fluctuations of amplitude and phase due to the presence of inhomogeneities are then described by the functions

$$\begin{aligned} \chi &= \ln \left| \frac{u}{u_0} \right| \\ \phi &= -i \ln \left(\frac{u}{u_0} \left| \frac{u_0}{u} \right| \right) \quad . \end{aligned} \quad (6)$$

In the weak fluctuation range the wavefield can be separated into a coherent and fluctuating (incoherent) part:

$$u = \langle u \rangle + u_f \quad , \quad (7)$$

where $\langle u \rangle$ denotes the ensemble averaged wavefield (meanfield). A measure of the wavefield fluctuations is the ratio

$$\varepsilon = \left| \frac{u_f}{\langle u \rangle} \right| \quad . \quad (8)$$

This gives

$$\langle \varepsilon^2 \rangle = \frac{I_t}{I_c} - 1 \quad , \quad (9)$$

where

$$I_t = \langle |u|^2 \rangle \quad (10)$$

is the total intensity (which is set to unity), $I_c = |\langle u \rangle|^2$ is the coherent intensity. The range of weak fluctuation is defined by $\langle \varepsilon^2 \rangle \ll 1$; that means the coherent intensity is of the order of the total intensity.

Due to the fluctuating character of χ and ϕ , it is expedient to look for their expectation values. If we make use of equations (7) and (8), neglect terms higher than $O(\varepsilon^2)$

and average, we obtain from equations (6)

$$\begin{aligned}\langle \chi \rangle &= \ln \left| \frac{\langle u \rangle}{u_0} \right| - \frac{1}{4} \langle \varepsilon_u^2 + \varepsilon_u^{*2} \rangle \\ \langle \phi \rangle &= \phi_c - \phi_0 + \frac{i}{4} \langle \varepsilon_u^2 - \varepsilon_u^{*2} \rangle \quad ,\end{aligned}\quad (11)$$

where $\varepsilon_u = u_f / \langle u \rangle$ so that $|\varepsilon_u| = \varepsilon$ and ε^* means the complex conjugated quantity. Further, the coherent wavefield may be represented as $\langle u \rangle = \sqrt{I_c} \exp(i\phi_c)$; ϕ_c denotes the coherent phase.

When we calculate the variance (crossvariance) of these quantities and neglect again terms of order higher than $O(\varepsilon^2)$, we find:

$$\begin{aligned}\sigma_{\chi\chi}^2 &= \frac{1}{4} \langle (\varepsilon_u + \varepsilon_u^*)^2 \rangle = -\ln \left| \frac{\langle u \rangle}{u_0} \right| + \frac{1}{4} \langle \varepsilon_u^2 + \varepsilon_u^{*2} \rangle \\ \sigma_{\chi\phi}^2 &= \frac{i}{4} \langle \varepsilon_u^2 - \varepsilon_u^{*2} \rangle \quad .\end{aligned}\quad (12)$$

Finally, with help of these second order moments we can express equations (11) as

$$\langle \chi \rangle = -\sigma_{\chi\chi}^2 \quad ,\quad (13)$$

$$\langle \phi \rangle = \phi_c - \phi_0 - \sigma_{\chi\phi}^2 \quad .\quad (14)$$

Equations (13) and (14) are derived here under the assumption of weak wavefield fluctuations (a more detailed derivation can be found in the papers cited above, see their equations (14) and (21)). Note that equations (13) and (14) can be also derived with the assumption of normally distributed random variables χ and ϕ . Furthermore, equation (13) follows directly from a second order Rytov approximation (see Rytov et al. (1987), equation (IV,2.111)). These relations are valid for both 2-D and 3-D random media.

In order to obtain a wave field representation of the form (5), we must now look for the quantities $\sigma_{\chi\chi}^2$, $\sigma_{\chi\phi}^2$ and ϕ_c . This task has been performed by Shapiro and Kneib (1993) (see their equations (28) and (29)) and by Shapiro et al. (1996b) (see equations (B12), (A16) and (A17)) for the 2-D case using the approach of Ishimaru (1978) and by Rytov et al. (1987) for the 3-D case. The results in 2-D media read

$$\begin{aligned}\sigma_{\chi\chi}^2 &= 2\pi k^2 L \int_0^\infty d\kappa \left(1 - \frac{\sin(\kappa^2 L/k)}{\kappa^2 L/k} \right) \Phi^{2D}(\kappa) \\ \sigma_{\chi\phi}^2 &= 4\pi k^3 \int_0^\infty d\kappa \left(\frac{\sin^2(\kappa^2 L/2k)}{\kappa^2} \right) \Phi^{2D}(\kappa) \\ \phi_c - \phi_0 &= 4\pi k^3 L \int_{2k}^\infty d\kappa \frac{\Phi^{2D}(\kappa)}{\sqrt{\kappa^2 - 4k^2}} \quad .\end{aligned}\quad (15)$$

For the 3-D case the results are:

$$\begin{aligned}
\sigma_{\chi\chi}^2 &= 2\pi^2 k^2 L \int_0^\infty d\kappa \kappa \left(1 - \frac{\sin(\kappa^2 L/k)}{\kappa^2 L/k} \right) \Phi^{3D}(\kappa) \\
\sigma_{\chi\phi}^2 &= 4\pi^2 k^3 \int_0^\infty d\kappa \kappa \left(\frac{\sin^2(\kappa^2 L/2k)}{\kappa^2} \right) \Phi^{3D}(\kappa) \\
\phi_c - \phi_0 &= \pi k^2 L \int_0^\infty d\kappa \kappa \ln \left(\frac{2k + \kappa}{2k - \kappa} \right)^2 \Phi^{3D}(\kappa) \quad .
\end{aligned} \tag{16}$$

In these equations $\Phi^{2D}(\kappa)$, $\Phi^{3D}(\kappa)$ denote the fluctuation spectra which are the 2-D and 3-D Fourier transforms of media correlation functions, respectively. The terms in brackets are the so-called spectral filter functions (since they act on the fluctuation spectra like filters; their behavior for the different wavefield ranges is discussed in Ishimaru, 1978). L means the travel-distance in the vertical direction and the background wavenumber is k ($k = \frac{\omega}{c_0}$, where c_0 is the constant background velocity). This means that the second-order medium statistics (controlled by $\Phi^{2D}(\kappa)$, $\Phi^{3D}(\kappa)$) are linked with the wavefield statistics ($\sigma_{\chi\chi}^2$, $\sigma_{\chi\phi}^2$). On the other hand the wavefield statistics are related to our wavefield representation Ψ via equations (13) and (14). These expressions can be simplified in the case of exponential and gaussian correlated fluctuations. An extension of these results to the case of anisotropic random media, characterized by anisotropic spatial correlation functions, should generally be possible.

The validity range of these approximations are weak wavefield fluctuations and inhomogeneities with spatial sizes of the order or larger than the wavelength (dominance of the forward scattering). Weak fluctuations mean that the log-amplitude variance is smaller than 0.5. The restriction of the crossvariance of log-amplitude and phase fluctuations is less stringent (see Ishimaru (1978) for a detailed discussion).

Self-averaging of logarithmic wavefield attributes

Applying the above results to single seismograms is only reasonable if we assume that logarithmic wavefield attributes undergo a self-averaging process when propagating through the random medium. A self-averaged quantity tends to its mathematical expectation value provided that the wave has covered a sufficient large distance inside the medium. In other words, if we can show that our theory is based upon self-averaged quantities, then the theoretical result will describe any typical and representative single realization of a seismogram. A sound investigation of the self-averaging phenomena can be found in Lifshits et al. (1988). For 1-D random media, it can be shown that the attenuation coefficient as well as the vertical phase increment of the transmissivity are such self-averaged quantities (Shapiro and Hubral, 1999).

For 2-D and 3-D media, we do this by showing that the attenuation coefficient $\alpha = -\frac{\chi}{L}$ as well as the phase increment $\varphi = \frac{\phi}{L} + k$ in the above discussed approximations tend to their expectation values for increasing travel distances. In analogy to the 1-D case, we compute the relative standard deviations of the attenuation coefficient and phase increment and find the rough estimates

$$\frac{\sigma_\alpha}{\alpha} \approx \sqrt{\frac{1}{\alpha L}} \propto \sqrt{\frac{1}{L}} \quad (17)$$

$$\frac{\sigma_\varphi}{\varphi} \approx \frac{\sqrt{\sigma_{\phi\phi}^2}}{\phi_0} \propto \sqrt{\frac{1}{L}} \quad , \quad (18)$$

where

$$\sigma_{\phi\phi}^2 = 2\pi k^2 L \int_0^\infty d\kappa \left(1 + \frac{\sin(\kappa^2 L/k)}{\kappa^2 L/k} \right) \Phi^{2D}(\kappa) \quad , \quad (19)$$

for 2-D media (see equation 17-52 in Ishimaru (1978) for the 3-D expression). It is obvious that for increasing travel-distance, the relative standard deviations decrease like $1/\sqrt{L}$ and therefore the process of self-averaging takes place. We conclude that the logarithmic wavefield quantities under consideration are self-averaged quantities at least in the weak wavefield fluctuation region, where our description is valid.

The numerical demonstration of self-averaging is given in the following, where we use the results of plane wave transmission simulations (the finite difference experiment is described in detail in section (3.1)):

The phase velocity of a picked phase is given by $v = \frac{L}{\langle t \rangle}$ with traveltime t . Comparing this with equation (6) in Shapiro et al. (1996), we see that fluctuations of the traveltime are proportional to the fluctuations of the phase increment. Therefore it is possible to demonstrate the self-averaging of φ by looking at the relative traveltime fluctuations. So we consider the measured traveltime fluctuations versus the spatial position transverse to the main propagation direction for different travel-distances L . Figure (1) shows the relative fluctuations of the traveltimes that are measured at 54 geophones along receiver-lines located at three different depths inside the random medium. We clearly observe that for increasing travel-distances, the relative traveltime fluctuations decrease. Computing the relative standard deviations of the traveltimes $\sqrt{\sigma_t^2}/\langle t \rangle$ for several travel-distances yields the theoretically obtained $1/\sqrt{L}$ dependency. Analogously, we consider the attenuation coefficient α . It is numerically determined by the logarithmic increment of a Fourier transformed trace (with a constant time window) at the fundamental frequency of the input wavelet. Again we could observe the diminishing fluctuations for larger travel-distances like in Figure (1).

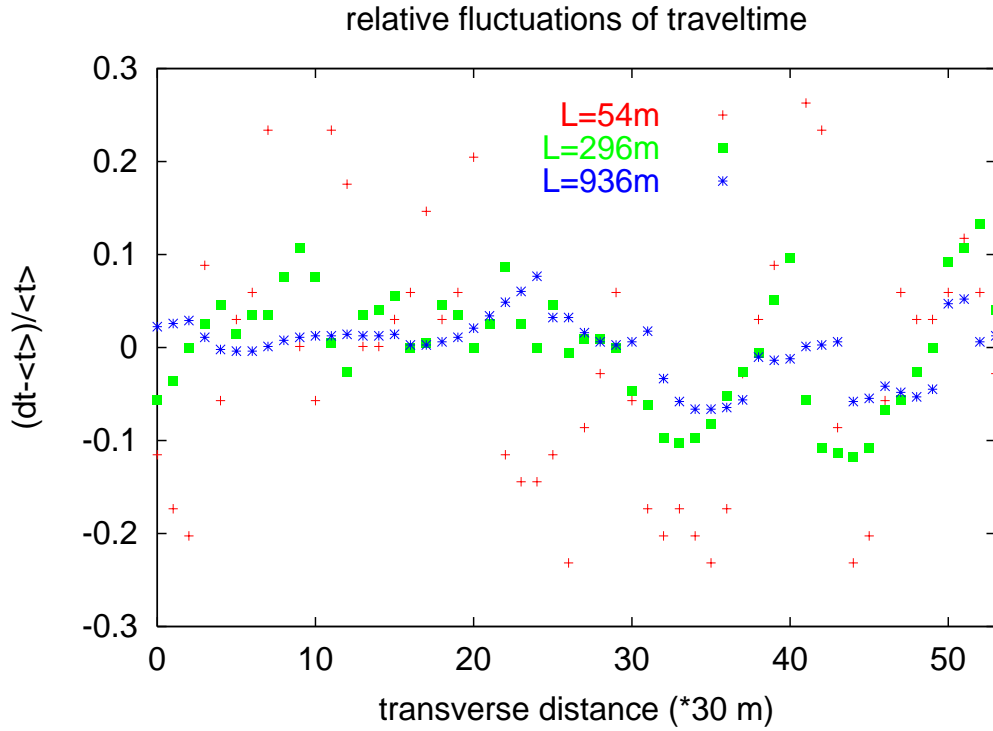


Figure 1: Relative fluctuations of the traveltimes recorded at 54 geophones along a receiver-line for three different depths. For increasing travel-distances the relative fluctuations become smaller.

Green's function for acoustic random media

By analogy with the 1-D situation, for wavefields in single typical realizations of 2-D and 3-D random media we will accept the following approximation of equation (5):

$$u_{appr} = u_0 e^{\langle \chi \rangle + i \langle \phi \rangle} \quad . \quad (20)$$

Therefore, in order to construct the Green's function we have to combine the results for the ensemble-averaged log-amplitude and phase fluctuations obtained in equations (13) and (14). Finally, by integration over the whole range of frequencies (an inverse Fourier transform) we obtain the time-dependent transmission response due to the initial plane wave:

$$G(t, z = L) = \frac{1}{2\pi} \int_{-\infty}^{\infty} d\omega e^{\langle \chi \rangle + i \langle \phi \rangle} e^{i(kL - \omega t)} \quad (21)$$

$$= \frac{1}{2\pi} \int_{-\infty}^{\infty} d\omega e^{i(KL - \omega t)} \quad (22)$$

with the complex wavenumber

$$K = \varphi + i\alpha \quad . \quad (23)$$

That is what we call the Green's function for random media; it is a real function since its Fourier transform consists out of an even real part and an odd imaginary part (see equations (15)-(16)).

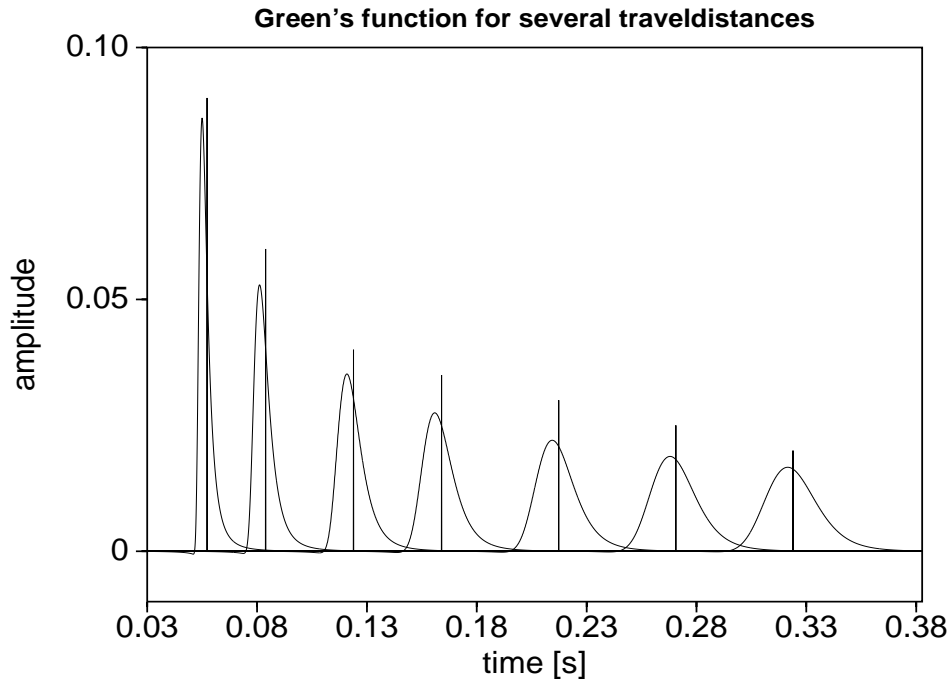


Figure 2: Green's function for several travel-distances. The pulses from left to right denote the transmission response of the exponential random medium (the standard deviation of the velocity fluctuations is 15%, the correlation length is 40m) due to a unit-pulse excitation for the travel-distances $L = 176, 256, 376, 496, 656, 816, 976$ m, respectively. For increasing travel-distances the amplitudes decrease and we observe a pulse broadening. This is the expected behavior since in (non-absorbing) heterogeneous media we deal with scattering attenuation. The vertical line nearby each pulse denotes the traveltime in the corresponding homogeneous (averaged-velocity) reference medium.

In Figure (2) we depict this Green's function for several travel distances assuming an 2-D exponentially correlated random medium. We can clearly observe the decrease of the transmission response for increasing travel-distances. This is only due to scattering attenuation. We observe also the broadening of the response.

In general, equation (21) can be easily evaluated using a FFT-routine.

It is now possible to describe seismic pulses as

$$u(t, z = L) = \frac{1}{2\pi} \int_{-\infty}^{\infty} d\omega U(\omega) e^{i(KL - \omega t)} \quad , \quad (24)$$

where $U(\omega)$ is the Fourier transform of the input signal. Due to the use of averaged wavefield attributes $\langle \chi \rangle$ and $\langle \phi \rangle$ (instead of χ and ϕ) in equation (20), we give a description of the main part of the transmitted pulse. To be specific, equation (24) describes the wavefield around the primary arrivals. We will confirm this by numerical simulations. Later arrivals, i.e. coda are not predicted within this approximation.

Green's function in elastic random media

Gold (1997) discussed the generalizations of the Rytov as well as the Bourret approximations to elastic media. He showed by a perturbation approach – analogous to the derivation of Ishimaru (1978, chapter 17)– that the exponent Ψ is exactly the same as in acoustic random media. Therefore, under the assumption of weak wavefield fluctuations, the propagation of elastic waves shows the same behaviour as acoustic waves. The Rytov approximation for elastic P and S-waves yields for the complex exponent Ψ in 2-D and 3-D random media the following equation:

$$\Psi_{P,S}^{2D,3D} = 2 \left(\frac{\alpha^2}{\beta^2} \right) \int n_v(\mathbf{r}') \frac{u_0(\mathbf{r}')}{u_0(\mathbf{r})} G^{2D,3D}(\mathbf{r} - \mathbf{r}') d\mathbf{r}' \quad , \quad (25)$$

where $G^{2D,3D}$ is the acoustic Green's function in 2-D/3-D and α, β are the P- and S-wavenumbers, respectively. This is exactly equation (17-19) of Ishimaru (1978) which states the first Rytov approximation for acoustic media and is the starting point in order to obtain equations (15)-(16).

Gold et al. (1999) applied the Bourret approximation in the Dyson equation in order to obtain the coherent Green's function in isotropic elastic media. From this consideration the coherent phase ϕ_c is obtained and can be used for equation (14). The results are more complicated, but can be evaluated by numerical integration.

To conclude, the strategy of the previous section can be used to construct the Green's function of elastic random media. More precisely, the amplitude level variance as well as the crossvariance of amplitude level and phase fluctuations can be used without modification. Therefore, the results obtained for acoustic waves can also be applied with slight modification to elastic media.

NUMERICAL EXPERIMENTS

FD-modeling in elastic random media

Now let us compare the analytical Green's function with finite difference simulation results for wave propagation in 2-D elastic (isotropic) random media with gaussian and exponential correlation functions. We use the so-called rotated-staggered grid finite difference scheme for the elastodynamic wave equation (Saenger et al., 2000).

In the present examples we simulate a plane wave propagating from the top down to a certain depth (z-direction) in a single random medium realization. The geometry as well as the medium parameters are of the order of reservoir scales and reservoir rocks, respectively.

The background medium is characterized by a P-wave velocity of 3000 m/s, a S-wave velocity of 1850 m/s and a density of 2.5 g/cm³. We choose the model geometry in such a way that undesired reflections from the model borders are excluded. For the modeling we need instead of velocities the stiffness tensor components $c_{11} = \lambda + 2\mu$ and $c_{55} = \mu$ (and density). For simplicity, only the stiffness tensor component c_{11} exhibits exponentially correlated fluctuations (the correlation length is 40 m, the corresponding standard deviation of the P-wave velocity is 15%). We use a body-force linesource with only a z-component. Note that under these conditions no S-waves will be generated. The wavelet is the second derivative of a Ricker-wavelet with a dominant frequency of about 75 Hz (this corresponds to a wavelength of 40 m for the P-wave). Furthermore, we fulfill the stability and dispersion criteria required for the rotated staggered grid in each point of the random medium.

Future work will be spent on modeling more complex media (fluctuating all Lamé-parameters and density, using a von Karman correlation function). For the moment, we think that the main features of the proposed theory are clearly demonstrated with help of these simple finite difference experiments. Accurate FD-modeling in 3-D elastic random media is still a fairly hard task in spite of the use of large parallel computer facilities.

What represents the Greens function in 2-D media?

Each gray 'background' in Figure (3) consists of 54 traces (the z-component of the wavefield) recorded on a common travel-distance gather at the corresponding depths 16, 96, 176, 256 and 336m. The distances between geophones along the receiver line is of the order of the correlation length so that statistically correlated measurements are avoided. From the uppermost to the lowermost seismograms in Figure (3) we clearly

Pulse propagation in random media

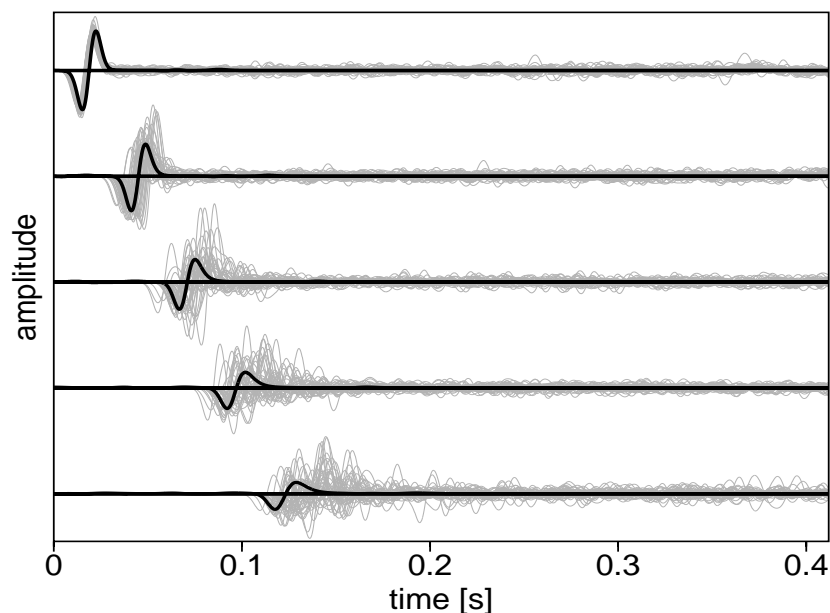
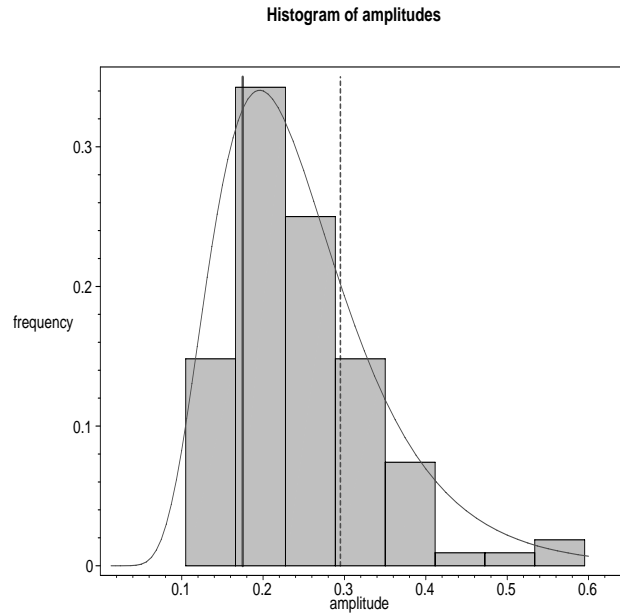


Figure 3: Comparison of FD-experiment and statistical wavefield description. In the background of each seismogram are displayed the traces recorded along the receiver-line (common travel-distance gather) at the depths 16,96,176,256 and 336m. The thicker, black curves denote the results of convolution of the corresponding Green's function with the input-wavelet.

observe that the amplitude as well as traveltimes fluctuations of traces – recorded at the same depths – increase with increasing travel-distances. This is physically reasonable since for larger travel-distances there are more interactions (scattering events) between wavefield and heterogeneities resulting in a more complex wavefield and consequently in more variable waveforms along the transverse distance of the main propagation direction. Note the increasing codas for larger travel-distances. The thicker black curve denotes the result of convolving the analytically computed Green's function with the input-wavelet $w(t)$ in the time domain: $u_z(t, z) = G(t, z) \star w(t)$. It is obvious that the theoretically predicted wavefield represents the simulated wavefield in a somehow averaged form. Thus, our formalism allows to model the evolution of seismic waves in random media near the first arrivals.

Moreover, the analytical curves give estimates of the primary wavefields for representative, 'typical' single traces. To be specific, typical realizations are defined to be close to the most probable realization (which in turn is defined by the maximum of

Figure 4: Histogram for the amplitudes of the primary wavefield measured (at 108 geophones located in the transverse direction of propagation) after travelling 336m in the random medium. The grey bars denote the probability for measuring certain amplitudes. A suitable probability density function is the log-normal distribution (black curve). The black vertical line denotes the amplitude predicted by our theory. The latter coincides with the maximum of the probability density function. The dashed vertical line denotes the amplitude value obtained by averaging over all measured amplitudes.



the probability density function). Figure (5) shows typical single seismograms at the depths 16, 96, 176, 256, 336m. The black curves denote the theoretically predicted wavefield for these travel-distances. To demonstrate that the simulated seismograms are typical ones, we consider the histogram of the amplitudes for all traces recorded at each travel-distance (see Figure (4) for the travel-distance $L = 336m$). So, the traces in Figure (5) are selected in such a way that their amplitudes are the most probable ones. We observe an excellent agreement between theory and experiment for the primary arrivals. Thus, using averaged logarithmed wavefield attributes for the construction of the Green's function, we give a description of the main part of the transmitted signal.

CONCLUSIONS

We consider a time-harmonic plane wave traveling through a random medium which is assumed to be an appropriate model of reservoirs and large regions of the lithosphere. These media are characterized by statistically homogeneous velocity fluctuations as well as by a spatial correlation function. With help of the Rytov approximation of the logarithmic wavefield we obtain a description of the wavefield which takes into account multiple forward scattering. Applying the inverse Fourier transform we get the wavefield due to a delta-pulse excitation. In other words, we obtain the Green's functions for 2-D and 3-D random media, taking into account the effects of small-scale heterogeneities. Numerical experiments show that with help of these

Pulse propagation in random media

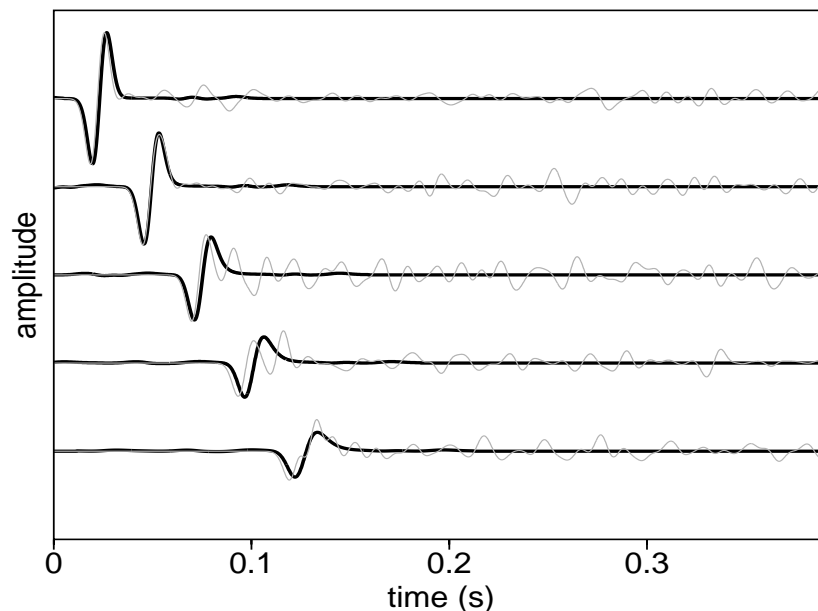


Figure 5: Pulse propagation in an exponential random medium: the present wavefield description is able to predict the wavefield around the primary arrivals of typical single realizations of seismograms. The thicker black curves denote the theoretically predicted wavefield (after travelling 16, 96, 176, 256, 336m), whereas the thinner gray curves denote the corresponding typical seismograms of a finite difference experiment in a exponentially correlated random medium with $a = 40\text{m}$, $\sigma_n = 0.15$ and $c_0 = 3000\text{m/s}$. The dominant frequency of the input wavelet is 75Hz, so that $ka \approx 2\pi$.

Green's functions, it is possible to predict a smooth version of primary arrivals of the transmitted wavefield from single realizations of seismograms. The results can be useful for modeling, imaging as well as for inverse problems.

REFERENCES

- Gold, N., 1997, Theoretical and numerical description of the propagation of elastic waves in random media: Ph.D. thesis, University of Karlsruhe.
- Ishimaru, A., 1978, Wave propagation and scattering in random media: Academic Press Inc.

- Lifshits, J. M., Gredeskul, S. A., and Pastur, L. A., 1988, Introduction to the theory of disordered systems: John Wiley & Sons.
- Rytov, S. M., Kravtsov, Y. A., and Tatarskii, V. J., 1987, Principles of statistical radio-physics: Springer, New York.
- Saenger, E. H., Gold, N., and Shapiro, S. A., 2000, Modeling the propagation of elastic waves using a modified finite-difference grid: *Wave Motion*, **31**, 77–92.
- Sato, H., and Fehler, M., 1998, Wave propagation and scattering in the heterogenous earth: AIP-press.
- Shapiro, S. A., and Hubral, P., 1999, Elastic waves in random media: Springer.
- Shapiro, S. A., and Kneib, G., 1993, Seismic attenuation by scattering: theory and numerical results: *Geophys. J. Int.*, **114**, 373–391.
- Shapiro, S. A., Schwarz, R., and Gold, N., 1996, The effect of random isotropic inhomogeneities on the phase velocity of seismic waves: *Geophys. J. Int.*, **127**, 783–794.
- Widmaier, M., Shapiro, S. A., and Hubral, P., 1996, Avo correction for a thinly layered reflector overburden: *Geophysics*, **61**, 520–528.
- Wu, R. S., 1982, Mean field attenuation and amplitude attenuation due to wave scattering: *Wave Motion*, **4**, 305–326.